1521-009X/46/5/514–524$35.00
Drug Metabolism and Disposition
https://doi.org/10.1124/dmd.117.079921
Drug Metab Dispos 46:514–524, May 2018

Post-transcriptional Regulation of UGT2B10 Hepatic Expression and Activity by Alternative Splicing [S]

Adrien Labriet, Eric P. Allain, Michèle Rouleau, Yannick Audet-Delage, Lyne Villeneuve, and Chantal Guillemette

Pharmacogenomics Laboratory, Centre Hospitalier Universitaire de Québec Research Center and Faculty of Pharmacy, Québec, Canada Research Chair in Pharmacogenomics, Université Laval, Québec, Canada

Received December 21, 2017; accepted January 31, 2018

ABSTRACT

The detoxification enzyme UDP-glucuronosyltransferase UGT2B10 is specialized in the N-linked glucuronidation of many drugs and xenobiotics. Preferred substrates possess tertiary aliphatic amines and heterocyclic amines, such as tobacco carcinogens and several antidepressants and antipsychotics. We hypothesized that alternative splicing (AS) constitutes a means to regulate steady-state levels of UGT2B10 and enzyme activity. We established the transcriptome of *UGT2B10* in normal and tumoral tissues of multiple individuals. The highest expression was in the liver, where 10 AS transcripts represented 50% of the *UGT2B10* transcriptome in 50 normal livers and 44 hepatocellular carcinomas. One abundant class of transcripts involves a novel exonic sequence and leads to two alternative (alt.) variants with novel in-frame C termini of 10 or 65 amino acids. Their hepatic expression was highly variable among individuals, correlated with canonical transcript levels, and was 3.5-fold higher in tumors. Evidence for their translation in liver tissues was acquired by mass spectrometry. In cell models, they colocalized with the enzyme and influenced the conjugation of amitriptyline and levomedetomidine by repressing or activating the enzyme (40%–70%; $P < 0.01$) in a cell context–specific manner. A high turnover rate for the alt. proteins, regulated by the proteasome, was observed in contrast to the more stable UGT2B10 enzyme. Moreover, a drug-induced remodeling of *UGT2B10* splicing was demonstrated in the HepaRG hepatic cell model, which favored alt. variants expression over the canonical transcript. Our findings support a significant contribution of AS in the regulation of UGT2B10 expression in the liver with an impact on enzyme activity.

Introduction

N-linked glucuronidation is an important inactivation route for amine-containing drugs and xenobiotics (Kaivosaari et al., 2011; Kato et al., 2013). Two of the 19 UDP-glucuronosyltransferases (UGTs), UGT2B10 and UGT1A4, are the main drivers of N-linked glucuronidation (Chen et al., 2008a; Kerdpin et al., 2009; Kato et al., 2013). Long described as an orphan UGT, the discovery that UGT2B10 is crucial for the detoxification of tobacco carcinogens has raised much attention and rationalized the importance of characterizing this unique UGT (Chen et al., 2007, 2008b; Kaivosaari et al., 2007; Berg et al., 2010; Murphy et al., 2014). UGT2B10 is one of the main liver UGT enzymes based on mRNA [quantitative polymerase chain reaction (PCR) and deep RNA-sequencing data] and protein levels (quantitative mass spectrometry–based proteomics data) (Court et al., 2012; Fallon et al., 2013; Margaillan et al., 2015; Tourancheau et al., 2017). Expression has also been reported in the breast, testis, gallbladder, tongue, and tonsils, although at much lower levels than hepatic expression (Haakensen et al., 2010; Jones and Lazarus, 2014).

UGT2B10 displays a preference for tertiary aliphatic amines and heterocyclic amines. These structures are found in several clinically used drugs, such as antihistamines, antipsychotics, and antidepressants, including several of the tricyclic class such as imipramine and amitriptyline (Kaivosaari et al., 2008, 2011; Kato et al., 2013; Kazmi et al., 2015; Pattanawongsa et al., 2016), whereas endogenous substrates have yet to be identified. Although UGT1A4 substrate preference significantly overlaps with that of UGT2B10, the latter presents a greater affinity and clearance for many tertiary cyclic amines at a therapeutic concentration (Kato et al., 2013). One structural determinant of the specificity toward amine substrates may be the residues Pro40 of UGT1A4 and Leu34 of UGT2B10, located in their substrate binding domain, a position that is otherwise a strictly conserved histidine residue (His40, coordinates of UGT1A1) in all human UGTs (Kerdpin et al., 2009).

This work was supported by the Canadian Institutes of Health Research [FRN-42392] and the Canada Research Chair in Pharmacogenomics (Tier I); A.L. and E.P.A. were supported by graduate scholarships from the "Fonds d'enseignement et de recherche" of the Faculty of pharmacy, Laval University; Y.A.-D. was supported by a graduate scholarship from the "Fonds de Recherche du Québec - Santé." The Genotype-Tissue Expression Project was supported by the Common Fund of the Office of the Director of the National Institutes of Health, and by National Cancer Institute (NCI); National Human Genome Research Institute (NHGRI); National Heart, Lung, and Blood Institute; National Institute on Drug Abuse; National Institute of Mental Health; and National Institute of Neurologic Disorders and Stroke, and the Cancer Genome Atlas is managed by the NCI and NHGRI (http://cancergenome.nih.gov).

All authors declare they have no competing interest.

https://doi.org/10.1124/dmd.117.079921.

[S] This article has supplemental material available at dmd.aspetjournals.org.

ABBREVIATIONS: alt., alternative; AS, alternative splicing; BLAST, Basic Local Alignment Search Tool; CAR, constitutive androstane receptor; Endo, endoglycosidase; ER, endoplasmic reticulum; FXR, farnesoyl X receptor; G, glucuronide; GTEx, The Genotype-Tissue Expression; GW4064, 3-(2,6-Dichlorophenyl)-4-(3 -carboxy-2-chlorostilben-4-yl)oxymethyl-5-isopropylisoxazole; i4, isoform 4; i5, isoform 5; MG132, N-Benzyloxycarbonyl-L-leucyl-L-leucyl-L-leucinal; MRM, multiple reaction monitoring; MS, mass spectrometry; PCR, polymerase chain reaction; PXR, pregnane X receptor; RNA-seq, RNA sequencing; RO5263397, (S)-4-(3-fluoro-2-methyl-phenyl)-4,5-dihydro-oxazol-2-ylamine; SNP, single nucleotide polymorphism; TCGA, The Cancer Genome Atlas; UGT, UDP-glucuronosyltransferase.

Genetic studies of smokers have established a direct link between single nucleotide polymorphisms (SNPs) at the *UGT2B10* gene locus (4q13.2), UGT2B10 activity, and metabolism of nicotine and cotinine (Chen et al., 2007, 2012; Murphy et al., 2014; Patel et al., 2015; Ware et al., 2016; Murphy, 2017). Two relatively frequent polymorphisms are associated with significantly decreased nicotine and cotinine glucuronidation in humans. One variant creates the missense Asp67Tyr coding variant (rs61750900) that abolishes UGT2B10 glucuronidation activity (Chen et al., 2007), whereas the other variant (rs116294140/rs2942857) alters the splice acceptor site between intron 2 and exon 3, and is thought to create an unstable mRNA (Murphy et al., 2014; Fowler et al., 2015). Consistently, individuals homozygous for either of these SNPs have very low to undetected nicotine and cotinine glucuronides in urine, further indicating that UGT2B10 is the main UGT responsible for glucuronidation of nicotine and cotinine (Chen et al., 2007; Murphy et al., 2014). This also supports the main role of the detoxification pathway in tobacco carcinogenesis. These genetic variations display an important ethnic bias. Whereas the Asp67Tyr variation is most frequent in Caucasians (nearly 10%) (Chen et al., 2007; Murphy et al., 2014), the splice variant rs2942857 prevails in approximately 35% of African Americans and in up to 50% of subjects of African origins (https://www.ncbi.nlm.nih.gov/projects/SNP/snp_ref.cgi; Murphy et al., 2014). Of interest, the splice variant was also reported to affect the metabolism of the antipsychotic preclinical drug RO5263397 [(S)-4-(3-fluoro-2-methyl-phenyl)-4,5-dihydro-oxazol-2-ylamine], whose main clearance route is N-glucuronidation (Fowler et al., 2015). It is thus likely that these SNPs also affect the glucuronidation of prescribed drugs conjugated by UGT2B10, such as amitriptyline (Kaivosaari et al., 2008; Kato et al., 2013).

Recent studies by our group revealed that alternative splicing (AS) largely expands the UGT transcriptome (Tourancheau et al., 2016, 2017). In turn, alternative (alt.) isoforms modulate the activity of UGT enzymes, suggesting that AS programs may contribute to interindividual variability in xenobiotic metabolism and cancer susceptibility (Bellemare et al., 2010b; Menard et al., 2013; Rouleau et al., 2014, 2016). Given the clinical importance of UGT2B10, by virtue of its detoxification functions toward tobacco by-products, antidepressants, and antipsychotics, we hypothesized that AS represents a mean to regulate steady-state levels of UGT2B10 mRNA and enzyme activity. The goal of this study was to investigate, in more detail, the expression of UGT2B10 and evaluate the influence of alternative isoforms on the metabolic functions of UGT2B10.

Materials and Methods

Analysis of UGT2B10 mRNA Expression

To carefully analyze *UGT2B10* expression and AS patterns, raw RNA sequencing (RNA-seq) data were downloaded from public databases and realigned to the recently established UGT transcriptome [Tourancheau et al., 2016; The Genotype-Tissue Expression (GTEX) (http://www.gtexportal.org/home/) and The Cancer Genome Atlas (TCGA) (https://gdc.cancer.gov/)]. RNA-seq data sets were obtained from dbGaP at http://www.ncbi.nlm.nih.gov/gap through the database of Genotypes and Phenotypes (dbGaP) accession number phs000424.v6.p1, project ID 13346. The GTEx normal liver data (downloaded on June 7, 2017) were from 50 healthy individuals [29 males, 18 females, three unknown; median age: 55 years old (range 21–69 years old), mostly Caucasians]. The TCGA cancer liver data (downloaded on August 22, 2017), all hepatocellular carcinoma, were from 44 individuals [29 males, 15 females; median age: 62 years old (range 18–82 years old), 16 Caucasians, 22 Asians, and five African-Americans]. GTEx RNA-seq data for bladder ($n = 6$), breast ($n = 51$), colon ($n = 49$), lung ($n = 48$), kidney ($n = 35$), prostate ($n = 50$), and skin ($n = 53$) were similarly obtained. HepaRG RNA-seq data (GSE71446, accessed March 9, 2017) (Li et al., 2015) were downloaded from the National Center for Biotechnology Information (NCBI) gene expression omnibus database. For each individual RNA-seq data, quality of FASTQ files was assessed with FastQC (http://www.bioinformatics.babraham.ac.uk/projects/fastqc) before quality trimming with Trimmomatic version 0.36 (Bolger et al., 2014). UGT transcript quantification was done with trimmed reads from each sample and a custom UGT transcript annotation (Tourancheau et al., 2016) using Kallisto version 0.43 (Bray et al., 2016). Data (counts) were then upper-quantile normalized and further adjusted using housekeeping genes, as previously described (de Jonge et al., 2007), using the EDASeq (Risso et al., 2011) and RUVSeq (Risso et al., 2014) packages for R version 3.2.2. Differential expression of UGT isoforms was assessed using the edgeR package for R. Normalized counts were then converted to counts per million or transcripts per million using transcript length. Reverse-transcription PCR analysis of *UGT2B10* transcripts was performed as previously described (Tourancheau et al., 2016), using primer sequences provided in Supplemental Table 1. The Basic Local Alignment Search Tool (BLAST) of the NCBI (https://blast.ncbi.nlm.nih.gov/Blast.cgi) served to search sequence similarity between the novel UGT2B10 sequences and other genes in humans and other species. The Protein BLAST (blastp) suite was used to search "nonredundant protein sequences" and "reference proteins" whereas the translated nucleotide (tblastn) suite was used to search the "nucleotide collection" and "reference RNA sequences" with the unique amino acid sequences of alt. proteins.

Expression Vectors and Human Cell Models (HEK293 and HepG2)

To study alt. transcripts and proteins, expression vectors were produced from the *UGT2B10_v1* pcDNA6 construct (Beaulieu et al., 1998) using the Q5 Site-Directed Mutagenesis kit (New England Biolabs Ltd., Whitby, ON, Canada). Sequences of purified primers used for mutagenesis are provided in Supplemental Table 1. The UGT2B10_v1 coding sequence was also cloned in the pcDNA3.1 vector to produce coexpression cell models (discussed later). All constructs were verified by Sanger sequencing. For the expression of alt. proteins tagged with V5-his (for immunoprecipitation studies), the stop codon of each coding sequence cloned in the pcDNA6 vector was removed using the Q5 Site-Directed Mutagenesis kit to permit in-frame V5-his expression.

HEK293 and HepG2 cell lines were obtained from the American Type Culture Collection (Manassas, VA) and grown as previously described (Levesque et al., 1997; Menard et al., 2013). HEK293 cells (UGT negative; 2×10^6 cells in a 10-cm plate) were transfected with 1 μg of each construct using Effectene (Qiagen, Toronto, ON, Canada), and HepG2 cells (UGT positive; 1×10^7 cells) were transfected with 20 μg of each construct by electroporation with the Neon Transfection System (Invitrogen, Thermo Fisher Scientific, Ottawa, ON, Canada) as per the manufacturers' instructions. HEK293 cells stably expressing the UGT2B10 cDNAs were established by supplementing cell culture media with blasticidin (10 μg/ml; Wisent, St-Bruno, QC, Canada). Clones were selected based on UGT2B10 expression detected by immunoblotting with antibodies specified later. HEK293 cells coexpressing UGT2B10_v1 (encoding the canonical enzyme) and alt. UGT2B10 (with novel sequences in C termini) were established by subsequent transfection of HEK293 clones expressing alt. sequences with the UGT2B10_v1-pcDNA3.1 construct and selection with G418 (1 mg/ml; Invitrogen). HepG2 cells, which express UGT2B10_v1 endogenously, were transfected with the constructs expressing alt. variants, and clone selection was with blasticidin. Control HEK293 and HepG2 cells were produced by transfection with the parental vector pcDNA6 and selection as discussed earlier.

Analysis of Protein Expression

Antibodies. The rabbit polyclonal anti-UGT2B10 #1845, produced in house against GST-UGT2B11 (aa 60-140) by Dr. Alain Bélanger's group (Chouinard et al., 2006), was used for the immunodetection of UGT2B10 in HepG2 (1:5000) and HEK293 (1:10,000) cell models. Our analysis revealed that this antibody detects UGT2B10, UGT2B11, and less efficiently UGT2B28 (Supplemental Fig. 1). The monoclonal anti-UGT2B10 antibody (ab57685; Abcam, Toronto, ON, Canada) was used for immunoprecipitation in human liver. Cell compartment-specific antibodies used for immunofluorescence were anti-58K Golgi protein (1:100, ab27043; Abcam), anti-protein disulfide isomerase (1:100, ab2792; Abcam) for the endoplasmic reticulum (ER), and anti-lamin (1:200, sc-376248; Santa Cruz Biotechnology, Dallas, TX). DNA was stained with DRAQ5 (1:2000; Thermo Fisher Scientific). Anti-calnexin was from Enzo Life Sciences (ADI-SPA-860, 1:5000; Farmingdale, NY).

Mass Spectrometry–Multiple Reaction Monitoring. Detection of peptides unique to alt. UGT2B10 was as described (Rouleau et al., 2016) with minor modifications. In brief, human liver S9 fraction (8 mg of proteins Xenotech LLC, Lenexa, KS) was lysed for 45 minutes on ice in a total volume of 4 ml of Lysis Buffer containing 0.05 M Tris-HCl (pH 7.4), 0.15 M NaCl, 1% (w/v) Igepal CA-630 (Sigma-Aldrich, St. Louis, MO), 1 mM dithiothreitol, and complete protease inhibitor cocktail (Roche, Laval, QC, Canada). Lysates were centrifuged for 15 minutes at 13,000*g*, and UGT2B10 was immunoprecipitated with 10 μg of the monoclonal anti-UGT2B10 (ab57685; Abcam) for 1 hour at 4°C on an orbital shaker. Protein complexes were captured by an overnight incubation at 4°C with protein G–coated magnetic beads (200 μl of Dynabeads; Thermo Fisher Scientific). Beads were washed in lysis buffer and with 50 mM ammonium bicarbonate and stored at −20°C until analysis. Tryptic digests of UGT2B10 were prepared and analyzed by mass spectrometry (MS)–coupled multiple reaction monitoring (MRM) on a 6500 QTRAP hybrid triple quadrupole/linear ion trap mass spectrometer (Sciex, Concord, ON, Canada) as previously described (Rouleau et al., 2016). In brief, MS analyses were conducted with an ionspray voltage of 2500 V in positive ion mode. Peptides were desalted on a 200-μm × 6-mm chip trap ChromXP C18 column, 3 μm (Eksigent; Sciex), at 2 μl/min solvent A (0.1% formic acid). Peptides were then eluted at a flow rate of 1 μl/min with a 30-minute linear gradient from 5% to 40% solvent B (acetonitrile with 0.1% formic acid) and a 10-minute linear gradient from 40% to 95% solvent B. MRM analyses were performed using the four most-intense transitions for each of the target peptides for the light and heavy forms. The UGT2B10 signature peptides were detected in tryptic digests of the immunoprecipitated UGT2B10 samples, and peptide identity was confirmed by coinjection of isotopically labeled [^{13}C6,^{15}N2]Lys and [^{13}C6,^{15}N4]Arg synthetic peptides (Pierce Protein Biotechnology, Thermo Fisher Scientific).

Glucuronidation Assays. For enzymatic assays in intact cells (*in situ* assays), two cell models were used (HEK293 and HepG2 cells). Cells were seeded in 24-well plates (HEK293: 8×10^4 cells/well; HepG2: 2.25×10^5 cells/well). Assays were initiated 48 hours after seeding by replacing the culture medium with fresh medium (1 ml/well) containing a UGT2B10 substrate (amitriptyline, 7.5 and 150 μM; levomedetomidine, 7.5 and 75 μM). All substrates were obtained from Sigma-Aldrich. Cells were incubated for 4 hours, and media were then collected and stored at −20°C until glucuronide (G) quantification by high-performance liquid chromatography–tandem mass spectrometry. Assays were replicated in at least two independent experiments in triplicates. Separation of amitriptyline and levomedetomidine was performed on an ACE Phenyl column 3 μM packing material, 100 × 4.6 mm (Canadian Life Science, ON, Canada). Isocratic condition with 70% methanol/30% water/3 mM ammonium formate with a flow rate of 0.9 ml/min was used to elute amitriptyline-G. A linear gradient was used to elute levomedetomidine-G, with 5% methanol/95% water/1 mM ammonium formate as initial conditions followed by a 10-minute linear gradient to 90% methanol/10% water/1 mM ammonium formate. The glucuronides were quantified by tandem mass spectrometry (API 6500; Biosystems-Sciex, Concord, ON, Canada). The following mass ion transitions (m/z) were used: 377.1 → 201.1 for levomedetomidine-G and 454.2 → 191.1 for amitriptyline-G. Glucuronidation activity (area/h/mg protein/UGT level) was normalized for the expression of the UGT2B10 enzyme in each cell model, determined by densitometry scanning of band intensity on immunoblots with antibody #1845. Cycloheximide glucuronidation assays were conducted using microsomes isolated from human liver (Xenotech LLC), HepG2-pcDNA6 described earlier, commercial supersomes expressing UGT1A and UGT2B isoenzymes (Corning, Woburn, MA), and microsomes of UGT2B11-expressing HEK293 prepared in house as previously described (Lepine et al., 2004). Glucuronidation assays were conducted at 37°C using 20 μg of membrane proteins and a final concentration of 200 μM cycloheximide (Sigma-Aldrich). Cycloheximide-G quantification was conducted as specified earlier for the UGT2B10 substrates, using a linear gradient with 10% methanol/90% water/1 mM ammonium formate as the initial conditions followed by a linear gradient to 85% methanol/15% water/1 mM ammonium formate in 5 minutes.

Immunofluorescence. Subcellular distribution of UGT2B10 enzyme and alternative isoforms was carried out in HEK293 cells stably expressing either protein and detected with the anti-UGT2B10 antibody #1845 (1:1000) as previously described (Rouleau et al., 2016).

Immunoprecipitation. Stable HEK293 *UGT2B10_v1* cells (2×10^6 cells) were seeded in 10-cm plates and transiently transfected with alt. UGT2B10 V5-tagged constructs (3 μg) using Effectene as per the manufacturer's instructions (Qiagen). Thirty-six hours post-transfection, cells were processed for cross-linking and immunoprecipitation with the polyclonal anti-V5 (1:600, NB600-380; Novus Biologicals, Littleton, CO) as previously described (Rouleau et al., 2016).

Protein and mRNA Stability in Cell Models. HEK293 cell models were seeded in six-well plates (4×10^5 cells/well) and grown for 48 hours. HepG2 cell models were seeded in six-well plates (1.5×10^6 cells/well) and grown for 24 hours. Cells were rinsed and incubated for 16 hours with media containing 1 μM MG132 (benzyl N-[(2S)-4-methyl-1-[[(2S)-4-methyl-1-[[(2S)-4-methyl-1-oxopentan-2-yl]amino]-1-oxopentan-2-yl]amino]-1-oxopentan-2-yl]carbamate) (Calbiochem, EMD Millipore, Etobicoke, ON, Canada) or vehicle (dimethylsulfoxide). Cells were harvested and protein extracts were prepared in Lysis Buffer. Cells were lysed for 30 minutes on a rotation unit, homogenized by pipetting up and down through fine needles (18G and 20G, 10 times each) on ice, and cleared by centrifugation for 15 minutes at 13,000*g* prior to analysis by immunoblotting using anti-UGT2B10 #1845. Duplicate cell samples were harvested for RNA extraction and reverse-transcription PCR analysis of UGT2B10 variants as previously described (Rouleau et al., 2016). Assays were performed twice. UGT2B10 protein half-lives were determined by treatment with cycloheximide (20 μg/ml) for 0–16 hours as previously described (Turgeon et al., 2003). Cells were washed in phosphate-buffered saline, collected, and lysed by scraping in lysis buffer prior to analysis by immunoblotting.

Assessment of the Glycosylation Status of UGT2B10 Proteins Expressed in HEK293 Cells. Microsomes (20 μg of proteins) prepared from HEK293 stably expressing each UGT2B10 isoform were treated with endoglycosidase (Endo) H and O-glycosidase obtained from New England Biolabs Inc. (Ipswich, MA) as previously described (Girard-Bock et al., 2016). Assays were performed in two independent experiments.

Results

***UGT2B10* Gene Expression Predominates in Human Liver and Is Regulated by Alternative Splicing.** For a quantitative assessment of *UGT2B10* expression, we performed a realignment of public GTEx and TCGA RNA-seq data from human tissue samples to the fully annotated UGT variant sequence database. This database was created based on RNA-seq experiments previously conducted with several human tissues (Tourancheau et al., 2016). Data indicated that the *UGT2B10* transcriptome is composed of one canonical and 10 alt. transcripts arising from the single *UGT2B10* gene. The *UGT2B10* alt. transcripts are created by partial intronization of exons 1–2, exon skipping of exons 4–6, and inclusion of novel terminal exons 6b or 6c. *UGT2B10* transcripts and encoded isoforms are depicted in Fig. 1. Data revealed *UGT2B10* as one of the highest expressed UGTs in normal liver samples, whereas variants arising from alternative splicing represented nearly 50% of the *UGT2B10* hepatic transcriptome (Fig. 2A). Some variant classes were remarkably abundant, with levels comparable to those of the canonical *UGT2B10_v1* transcript encoding the UGT2B10 enzyme—namely, those with N-terminal truncations and with novel C-terminal sequences (Fig. 2A). Total *UGT2B10* expression was 2.15-fold ($P = 0.013$) higher in hepatocellular carcinoma ($n = 44$) relative to normal livers ($n = 50$), and was highly variable among individuals (coefficients of variation of 93%–117%) (Fig. 2B). In contrast to the high hepatic levels, expression of *UGT2B10* in other normal tissues surveyed was much lower, with values below 1 transcript per million in the bladder, breast, colon, kidney, lung, prostate, and skin (data not shown).

Alternative Splicing Creates UGT2B10 Variants with Novel In-Frame C-Terminal Sequences Detected in Human Liver at the Protein Level. Splicing events generating *UGT2B10* transcripts (*n9* and *n10*) harboring novel C-terminal sequences were of particular interest for this study. These alt. variants are produced by intronization of parts of the canonical exon 6 and inclusion of a novel exon 6c (Fig. 1). These AS events appeared specific to humans and were not noted in other species based on BLAST searches in the nonredundant nucleotide collection and

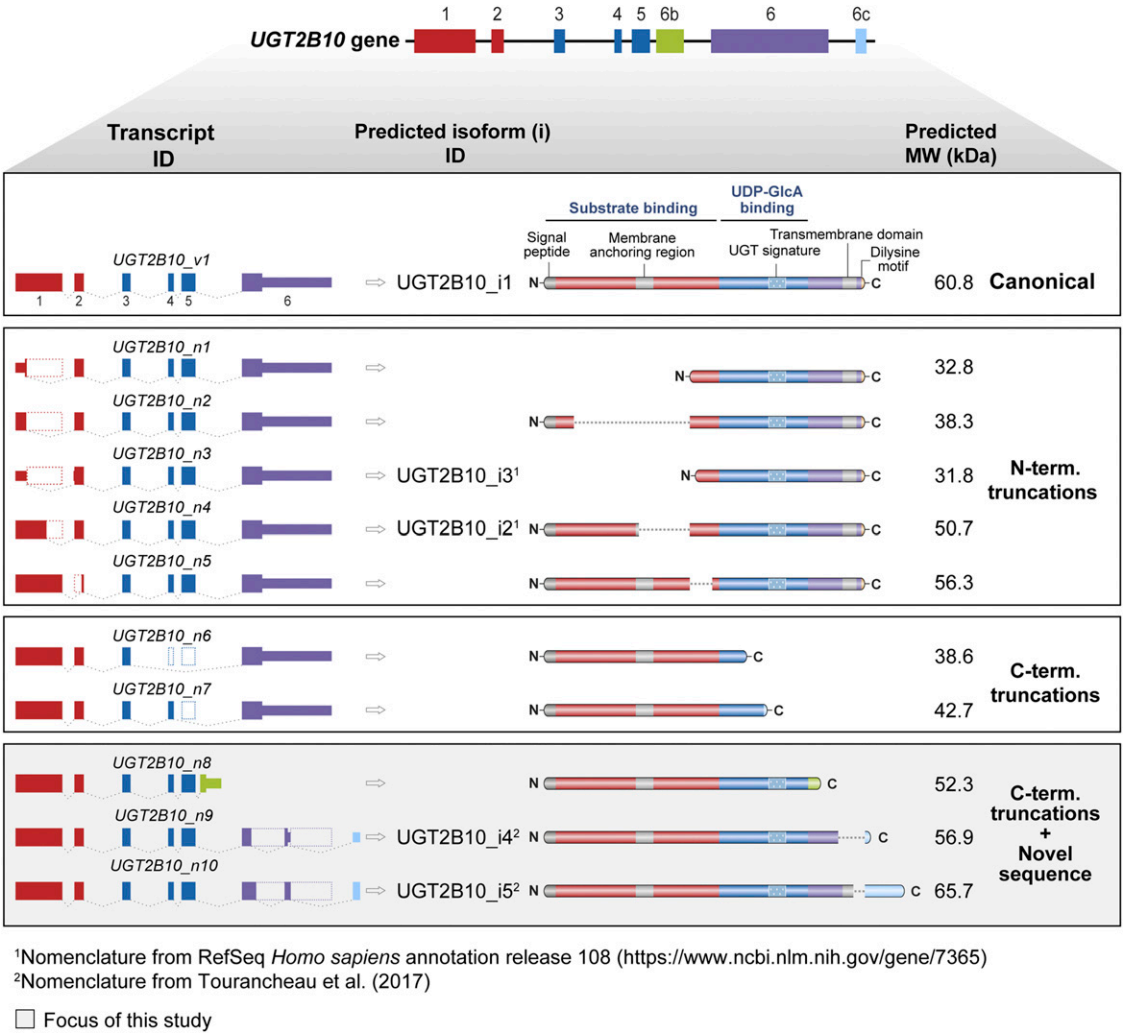

Fig. 1. Schematic overview of *UGT2B10* mRNA transcripts and encoded proteins. (Top) The *UGT2B10* gene is composed of six canonical exons and two alternative exons 6b and 6c. (Bottom) The canonical *UGT2B10_v1* transcript encodes the UGT2B10_i1 enzyme. Alternative splicing produces three classes of variants, with N-terminal or C-terminal truncations, and novel a C-terminal sequence. The N-terminally truncated *UGT2B10_n3* and *_n4* variants are reported in the NCBI RefSeq *UGT2B10* gene entry (https://www.ncbi.nlm.nih.gov/gene/7365) to encode isoforms i3 and i2, respectively, in RefSeq. Consequently, the isoform encoded by the transcripts *n9* and *n10* were named i4 and i5, respectively. Exons are represented by colored boxes and skipped exons by dashed boxes. Thinner parts of exons 1 and 6 represent untranslated regions. *UGT2B10* is the UGT2B with the largest 3′ untranslated region, and only the first 279 of 1424 nucleotides of exon 6 are coding in the canonical mRNA. Note that the predicted molecular mass (MW) of mature proteins is smaller by 2.5 kDa due to the cleavage of the signal peptide.

RNA reference sequence databases. Transcripts were abundant in human livers and were 3.5-fold higher in hepatic tumors relative to normal tissues. They represented, on average, 15% of total *UGT2B10* expression in normal liver tissues and 25% in hepatocellular carcinoma tissues (Fig. 2, A and B). The considerable interindividual variability for these alt. transcripts was higher than for the total and canonical *UGT2B10* hepatic expression. We also noted a significant positive correlation between the expression of the canonical and alt. transcripts ($\rho = 0.854$–0.915, $P \leq 0.001$) (Fig. 2C).

The putative UGT2B10 proteins encoded by these alt. transcripts are referred to as UGT2B10 isoforms 4 and 5, named i4 and i5, respectively. They are predicted to retain both the substrate and the cosubstrate (UDP-glucuronic acid) binding domains coupled to a novel alt. C-sequence (Fig. 1). Isoform 4 lacks the 43 C-terminal amino acids including the transmembrane domain and the positively charged C-terminal tail of the UGT2B10 enzyme that are replaced by 10 novel amino acids encoded by exon 6c (Fig. 3A). As for isoform 5, because a smaller portion of exon 6 is intronized, the encoded protein is predicted to retain 18 of the 24 transmembrane domain residues and to be extended by 65 novel amino acids, half of which are encoded by a frame shift in exon 6, and half by exon 6c (Fig. 1 and Fig. 3A).

Validation of endogenous protein expression was possible for UGT2B10_i5 through the identification of a unique peptide sequence by targeted MS-MRM of liver UGT2B10 immunoprecipitated from multiple donors (Fig. 3, B and C). This result is in line with the detection of the corresponding transcripts by PCR in human livers (Supplemental Fig. 2A). The endogenous expression of UGT2B10_i4 could not be addressed by this approach given the short and hydrophobic nature of the C-terminal unique sequence.

Alternative Isoforms with Novel C-Terminal Sequences Colocalized with the UGT2B10 Enzyme and Modified Its Activity In Vitro. The alt. UGT2B10 isoforms were stably expressed in the embryonic kidney cell line HEK293, devoid of endogenous UGT expression, alone or with the canonical UGT2B10 enzyme. In addition, their expression was examined in the liver cell model HepG2 that endogenously expresses the UGT2B10 enzyme and conjugates substrates of the enzyme, such as amitriptyline and levomedetomidine. We initially confirmed protein expression using immunoblot and immunofluorescence experiments using an anti-UGT2B10 antibody (#1845) that targets amino acids encoded by exon 1 and therefore recognizes the three UGT2B10

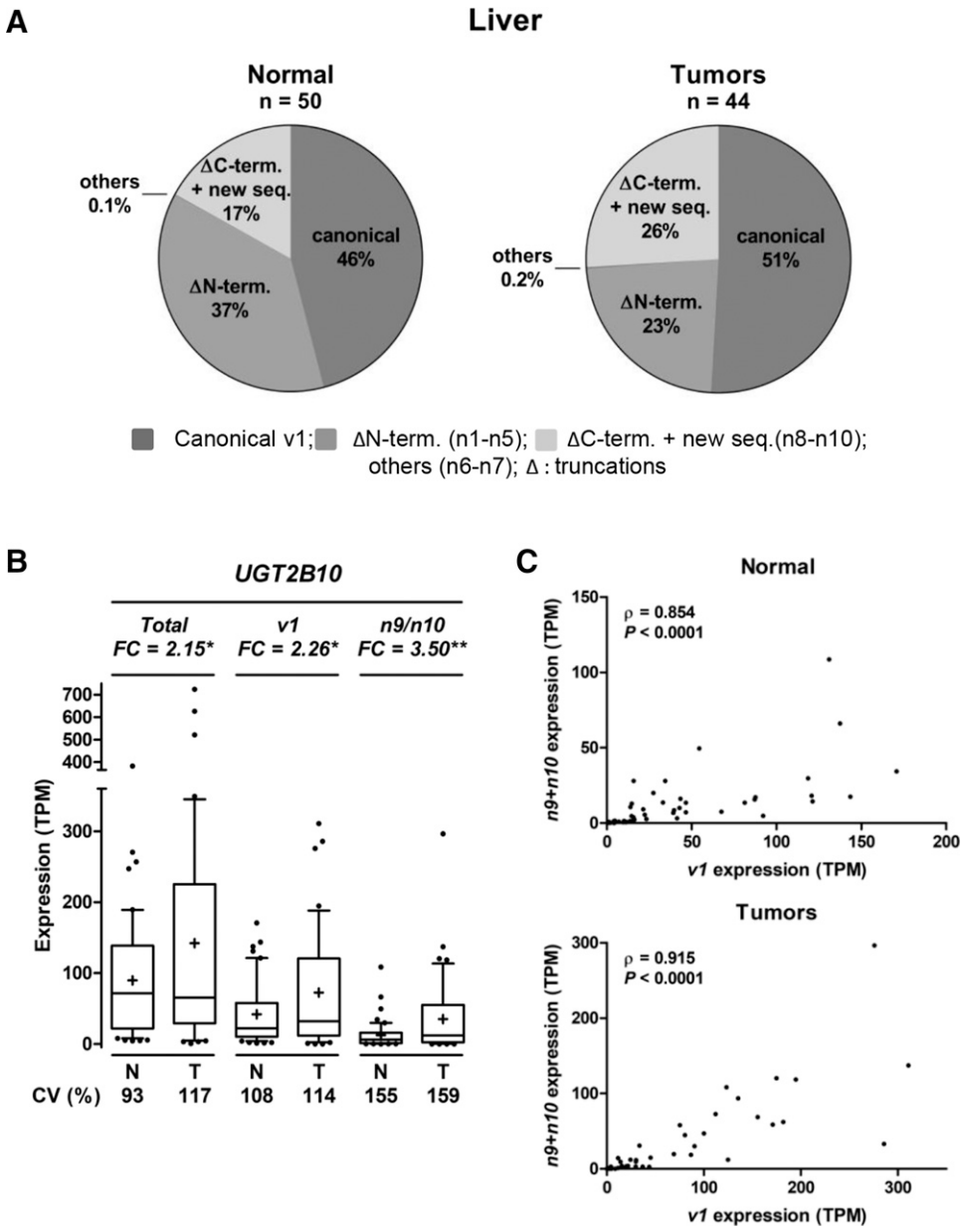

Fig. 2. Alternative splicing diversifies the hepatic *UGT2B10* transcriptome. (A) Relative levels of canonical (*v1*) and alt. transcript classes in the normal human liver and in hepatocellular carcinoma. The ΔC-term+new sequence class is predominantly composed of *n9* and *n10* transcripts, whereas transcript *n8* represents less than 2% in normal and tumor tissues. (B) Interindividual variability in *UGT2B10* expression for all transcripts (total), canonical (*v1*), and alt. transcripts (*n9/n10*). Boxes represent 25–75 percentiles, whiskers 10–90 percentiles. Median is indicated by the horizontal line and mean by a "+." (C) Correlation between *UGT2B10_v1* and *n9/n10* expression in normal livers and hepatocellular carcinoma. All expression data were derived by a realignment of RNA-seq data from GTEx (n = 50) and TCGA (n = 44) to the fully annotated UGT variant sequence (Tourancheau et al., 2016). CV, coefficient of variation; FC, fold change; N, normal tissues; T, tumor tissues; TPM, transcripts per million.

isoforms (Fig. 4A). Indeed, we detected UGT2B10_i4 and UGT2B10_i5 near their predicted molecular masses of 57 and 66 kDa in cell models (Fig. 4A).

The subcellular distribution of each protein was examined in the HEK293 models, where the canonical and alt. proteins were detected and largely restricted to an ER localization. This was confirmed by the colocalization with the ER marker protein disulfide isomerase (Fig. 4B). Each isoform also displayed minor perinuclear and Golgi localization (Supplemental Fig. 3). The glycosylation status of each protein was studied by subjecting microsomes from HEK293 cell models to Endo H glycosidase, which cleaves N-linked sugars on asparagine acquired by ER-resident enzymes, and to O-glycosidase, which removes serine and threonine O-linked complex sugars acquired in the Golgi. Each UGT2B10 protein was sensitive to Endo H treatment, revealed by the shift to a higher mobility protein band upon treatment (Fig. 4C). In contrast, their mobility was not affected by a treatment with O-glycosidase.

Enzymatic assays in intact cells were subsequently conducted in the hepatic cell model HepG2 that expresses the endogenous UGT2B10 enzyme. Compared with the reference cell line (stably transfected with pcDNA6), expression of alt. UGT2B10_i4 isoform enhanced the glucuronidation activity of the UGT2B10 enzyme with two drug substrates, amitriptyline and levomedetomidine, by 1.5- to 2-fold (Fig. 5, A and B). In turn, the presence of alt. UGT2B10_i5 significantly impaired the glucuronidation of amitriptyline and tended to reduce that of levomedetomidine as well by 20%–25%. Glucuronidation assays conducted with the UGT-negative HEK293 cells stably expressing either alt. UGT2B10 isoforms revealed no transferase activity for amitriptyline and levomedetomidine. When coexpressed with the UGT2B10 enzyme, we observed a significant 23%–65% inhibition of glucuronidation activity by HEK293 cells in the presence of the alt. i4 or i5 proteins (Fig. 5, A and B). Since we observed a colocalization of alt. isoforms and the UGT2B10 enzyme in the ER, we addressed their potential interaction as a possible regulatory mechanism. Immunoprecipitations were conducted with an anti-V5 epitope antibody using cell models stably expressing the UGT2B10 enzyme and transiently expressing either alt. isoform tagged with the V5 epitope. The UGT2B10

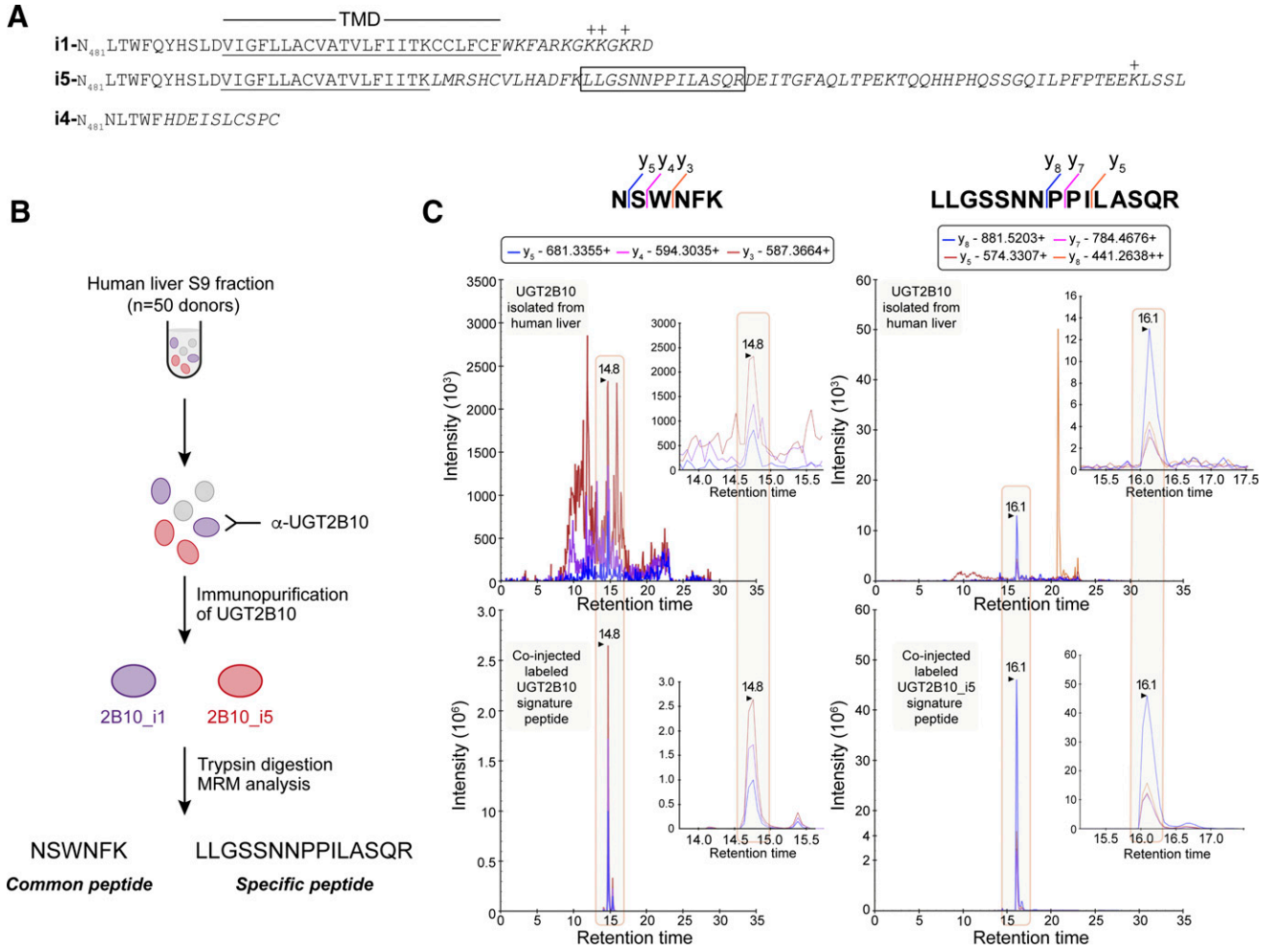

Fig. 3. Alternate UGT2B10 protein is expressed in the human liver. (A) C-terminal amino acid sequences of the UGT2B10 enzyme (i1) and alt. isoforms i4 and i5. Sequences unique to each alt. proteins are italicized. (B) Experimental approach for the detection of UGT2B10_i5 by immunoprecipitation and MRM. (C) The common UGT2B10 peptide NSWNFK (left) and the alt. specific peptide LLGSSNNPPILASQR (right) were detected in tryptic digests of UGT2B10 immunoprecipitated from human liver samples (upper chromatograms). The chromatograms of control peptides (lower chromatograms) labeled with stable isotopes mixed with the immunopurified UGT2B10 confirmed the identity of i1 and i5 peptides. Representative chromatograms are shown (n = 2). K̇, ER retention signal; TMD, transmembrane domain.

enzyme was immunoprecipitated with each alt. isoform, indicating their ability to form complexes (Fig. 5C).

Alternative Isoforms Have Shorter Half-Lives than the UGT2B10 Enzyme and Are Targeted for Degradation by the Proteasome. Protein stability was evaluated in both cell models. The UGT2B10 enzyme displayed a half-life over 16 hours in both HEK293 (exogenous expression) and HepG2 (endogenous expression) cell models, whereas the alt. isoforms displayed superior turnover rates. The alt. UGT2B10_ i5 was the least stable, with short half-lives of 1.9 and 0.7 hours in HEK293 and HepG2, respectively (Fig. 6A). The turnover rate of isoform i4 differed between the two cell models, and was 11.5 hours in HEK293 but much shorter in HepG2 (1.5 hours). In HepG2 cells, we noted a significant recovery of alt. protein expression, even rising above those of nontreated cells by 16 hours after initiation of the cycloheximide treatment. This was not observed for the UGT2B10 enzyme, nor for any of the UGT2B10 proteins in HEK293 cells. This observation implied a possible inactivation in HepG2 cells, which was confirmed by the detection of two glucuronides of cycloheximide (G1 and G2) with HepG2 microsomes (Supplemental Fig. 5). This was further validated using microsomal fractions of pooled human livers and UGT supersomes. In these experiments, UGT1A9 and UGT2B7 most efficiently glucuronidated cycloheximide (G1 and G2), whereas UGT1A3 and UGT1A4 (G1) as well as UGT1A1 and UGT2B4 (G1 and G2) also conjugated some cycloheximide (Supplemental Fig. 5), with some of them detected in HepG2 cells and not in the HEK293 cell model. As a consequence, this may lead to an inaccurate assessment of UGT protein half-lives using this approach in the HepG2 model.

Accordingly, the difference in protein stability between the UGT2B10 enzyme and alt. proteins was further addressed by proteasomal inhibition. Whereas the enzyme levels were nearly unperturbed by inhibition of the ubiquitin-proteasome system, alt. UGT2B10 and, more particularly, isoform i5 were stabilized, indicating that they were degraded via the ubiquitin-proteasome system. Proteasomal inhibition for 16 hours increased the ratio of alt. isoform/UGT2B10 enzyme in HepG2 liver cell models, whereas stabilization was more modest in HEK293 (Fig. 6B). Increased levels of alt. isoforms were not derived from enhanced transcription, verified at the mRNA level (Supplemental Fig. 2B).

Differential Induction of UGT2B10 Alternative Transcripts in Liver Cells by Phenobarbital and a Constitutive Androstane Receptor Agonist. HepaRG cells constitute a good surrogate system to study hepatic functions and response to drug treatments. An analysis of public HepaRG RNA-seq data (Li et al., 2015) with the exhaustive UGT transcriptome revealed an expression of canonical and alt. *UGT2B10* in

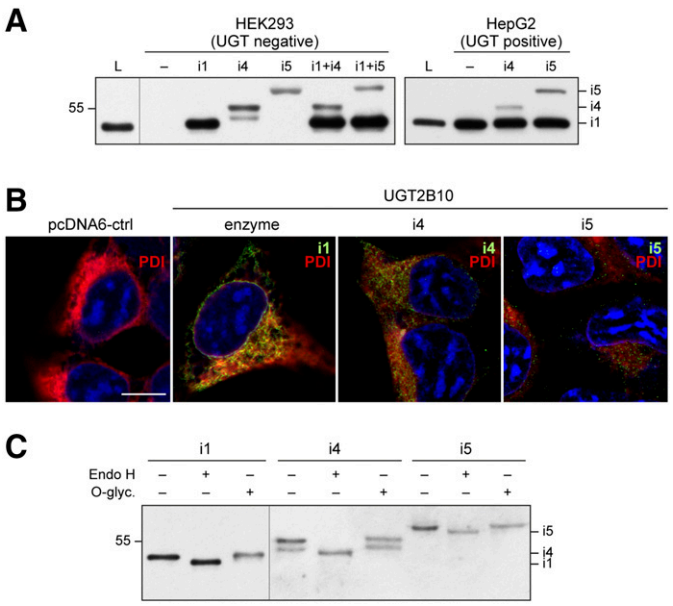

Fig. 4. Interaction of UGT2B10 isoforms in the ER. (A) Stable expression of UGT2B10 alternative isoforms in HEK293 and HepG2 cell models. UGT2B10 was detected in microsomal fractions of each cell model (20 μg of proteins) and of human liver (L) using the anti-UGT2B10 antibody. The expression ratio of the UGT2B10 enzyme relative to alt. isoforms is estimated to more than 4-fold in each model. Note that the apparent molecular mass of the enzyme was lower than predicted, likely explained by the influence of the hydrophobic amino acids in the transmembrane domains that perturb the interactions with SDS and the shape of the denatured protein (Rath et al., 2009). (B) UGT2B10 enzyme and alt. isoforms (i4 and i5) colocalized with the ER marker protein disulfide isomerase (PDI). Merged images of UGT2B10 proteins labeled with anti-UGT2B10 (green), PDI (red), and nuclei (blue) are shown. Separate images and colocalization with other subcellular markers are shown in Supplemental Fig. 3. Scale bar, 10 μm. (C) Glycosylation status of the UGT2B10 enzyme and alt. proteins. UGT2B10 proteins in microsomes from HEK293 cell models subjected to Endo H or O-glycosidase (O-glyc) were detected by immunoblotting.

comparable proportions to the human liver (not shown). In HepaRG cells treated with the constitutive androstane receptor (CAR) agonist CITCO [6-(4-chlorophen-yl)imidazo[2,1-b][1,3]thiazole-5-carbaldehyde-O-(3,4-dichlorobenzyl)oxime], a significant and preferential induction of the alt. UGT2B10 transcripts (1.4-fold, $P = 0.003$) occurred, whereas the enzyme-coding *v1* transcript was not significantly altered (Fig. 7). Phenobarbital did not significantly induce expression of *UGT2B10* in wild-type HepaRG cells. In contrast, in HepaRG cells with a CAR knockout, alt. transcripts were significantly upregulated by 1.8-fold ($P \leq 0.001$) by phenobarbital and 1.4-fold ($P = 0.011$) by the CAR agonist, whereas *v1* was not significantly perturbed (Fig. 7).

Discussion

The recent expansion of the pharmacogene transcriptome by AS has shed light on a novel mechanism regulating drug metabolism and clearance (Bellemare et al., 2010a,b; Guillemette et al., 2010, 2014; Rouleau et al., 2014, 2016; Chhibber et al., 2016; Tourancheau et al., 2016, 2017). Our study of the *UGT2B10* transcriptome, encoding a key detoxification enzyme specialized in N-glucuronidation of multiple harmful xenobiotics (Kaivosaari et al., 2007, 2011; Kato et al., 2013), demonstrated that AS accounts for a large proportion of *UGT2B10* gene expression, especially in the liver. This observation held true in liver tumors, where *UGT2B10* expression was enhanced 2-fold in hepatocellular carcinoma. Indeed, our analysis of next-generation sequencing data revealed that *UGT2B10* expression prevails in the liver, whereas in all other tissues surveyed, including the lung, its expression was low to undetected. This is consistent with the expression determined at the RNA level in several human tissues, including those of the aerodigestive tract (Ohno and Nakajin, 2011; Court et al., 2012; Jones and Lazarus, 2014). This supports that a main detoxification site of UGT2B10-dependent N-glucuronidation is the liver, where UGT2B10 is one of the most abundant UGT enzyme based on proteomics data (Fallon et al., 2013; Sato et al., 2014; Margaillan et al., 2015). In addition, AS also provides an explanation for the multiple observations reporting a lack of correlation between mRNA and protein expression, such as in hepatocellular carcinoma, where the RNA expression remained equivalent between tumor tissues and adjacent normal tissues, whereas glucuronidation activity was drastically decreased (Lu et al., 2015).

With a focus on one abundant class of hepatic alt. *UGT2B10* variants containing a novel 3′ terminal exon that were confirmed at the protein level in human liver samples and in heterologous expression models, we exposed their regulated expression and influence on UGT2B10 enzyme activity in vitro. In fact, the transcriptional regulation of *UGT2B10* has been poorly studied. A response element for the bile acid–sensing farnesoyl X receptor (FXR) was recently uncovered in the *UGT2B10* promoter region and participated in the induction of *UGT2B10* by the FXR agonists GW4064 (3-(2,6-Dichlorophenyl)-4-(3'-carboxy-2-chlorostilben-4-yl)oxymethyl-5-isopropylisoxazole) and chenodeoxycholic acid (Lu et al., 2017a). In the cell model HepaRG, a surrogate to human primary hepatocytes in drug-metabolism studies (Antherieu et al., 2012), RNA-seq data revealed drug-induced regulation of the *UGT2B10* transcriptome by both the CAR and pregnane X receptor (PXR). The superior induction of alt. *UGT2B10* by CAR and PXR agonists observed herein, especially in HepaRG cells devoid of CAR expression, further raises the possibility of a PXR-dependent remodeling of splicing events at the *UGT2B10* locus that may significantly influence UGT2B10 detoxification activity. Whether other receptors such as FXR, previously reported to regulate *UGT2B10* transcription (Lu et al., 2017a), also influence splicing remains to be addressed. When expressed in human cells, alt. UGT2B10 acted as a regulator of the glucuronidation activity of the UGT2B10 enzyme, possibly conveyed by heterologous complexes formed between the enzyme and alternative proteins, a regulatory mechanism documented for other human UGTs (Bushey and Lazarus, 2012; Menard et al., 2013; Rouleau et al., 2014, 2016). Our findings further suggest a cell-specific influence given that, in HepG2 cells, an increased N-glucuronidation of the UGT2B10 substrates amitriptyline and levomedetomidine by the endogenous enzyme was observed, in contrast with a repression of enzyme activity in HEK293 cells. The endogenous expression of additional UGTs other than UGT2B10 in HepG2 cells and different protein turnover rates could be among factors influencing their functions. Likewise, the impact of AS on UGT2B10 activity has been documented previously by findings of a common polymorphism (rs116294140) that disrupts a splice site in exon 3 and introduces a premature stop codon possibly triggering non-sense mRNA decay (Fowler et al., 2015). This polymorphism, particularly more frequent among African Americans, significantly reduced N-glucuronidation of drugs such as RO5263397 as well as nicotine and cotinine (Murphy et al., 2014; Fowler et al., 2015). In fact, occurrences of this splice site variant as well as the coding variant Asp67Tyr (rs61750900) were estimated to collectively explain over 24% of interindividual variability in cotinine glucuronidation (Patel et al., 2015). Our results support that alternative splicing at the *UGT2B10* locus may be a major factor contributing to this variability in the constitutive expression of the gene, with a potential impact on responses to substrates of the UGT2B10 pathway.

The alternate UGT2B10 proteins with novel in-frame C-terminal sequences are predicted to include the entire putative catalytic domain (Radominska-Pandya et al., 2010), although their enzyme activity could

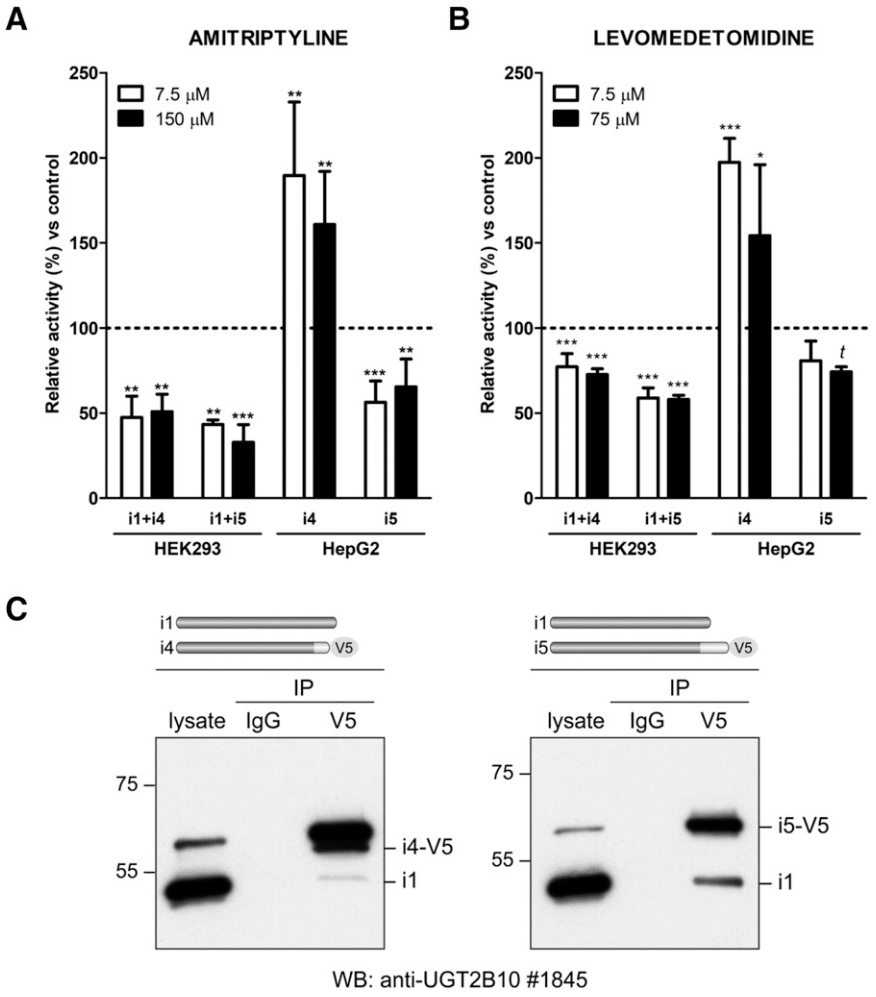

Fig. 5. The alternative UGT2B10 isoforms modulate the glucuronidation activity of the UGT2B10 enzyme. (A and B) *In situ* cell glucuronidation assays of amitriptyline and levomedetomidine in HEK293 and HepG2 cell models that coexpress the alt. isoforms i4 or i5. Activity is presented relative to that in cells expressing only the UGT2B10 enzyme (control). Assays were conducted twice in triplicates. *t*, $P \leq 0.1$; *$P \leq 0.05$; **$P \leq 0.01$; ***$P \leq 0.001$. (C) Coimmunoprecipitation of the UGT2B10 enzyme with alt. isoforms i4 and i5 expressed in HEK293. Alternative isoforms were C-terminally tagged with the epitope V5 and immunoprecipitated (IP) with the anti-V5 antibody. WB, Western blot.

not be confirmed in standard in vitro assay conditions when expressed in HEK293 human cells. This could be due to an inadequate topology of the alt. proteins essential for enzyme function. *In silico* analysis of the novel exonic sequence with NCBI BLAST tools did not reveal a match with other nucleotide or amino acid sequences of any organism. The splicing event at the *UGT2B10* locus appears specific to humans. This is consistent with the low to undetectable activity toward preferred UGT2B10 substrates such as N-heterocyclic amines and aliphatic tertiary amines in most primates and other mammals, suggesting that *UGT2B10* expression occurs preferentially in humans (Kaivosaari et al., 2007, 2008; Zhou et al., 2010; Lu et al., 2017b). The novel appended amino acid sequence encoded in the alternative frame by exon 6 is, however, related to that of putative alternative variants of several other human proteins, including CLCN3 (chloride exchange transporter 3), ALG9 (alpha-1, 2-mannosyltransferase), and CHFR (E3-ubiquitin ligase), supporting that the new sequence may encode a conserved domain (Supplemental Fig. 6).

As for subcellular localization, our immunofluorescence data indicated that the alt. isoforms, partially or completely lacking the transmembrane domain and devoid of the positively charged lysine tail (Fig. 3), are nonetheless ER-resident proteins when expressed in HEK293 human cells. Although studied in a limited set of UGTs, the high sequence similarity of ER retention elements among UGTs supports a common ER retention mechanism. ER residency of UGT enzymes is mediated by at least four protein regions: the N-terminal signal peptide, a short hydrophobic patch in the N-terminal substrate binding domain, the C-terminal transmembrane region, and the cytoplasmic dilysine motif containing the ER retention signal "KXKXX" (K, lysines; X, any amino acids) (Jackson et al., 1993; Ciotti et al., 1998; Ouzzine et al., 1999; Barre et al., 2005). In line with our observations, these structural features may be partially redundant, as none appears strictly essential to ER retention. The Endo H sensitivity and lack of sensitivity toward O-glycosidase for the UGT2B10 enzyme and alt. UGT2B10 also support ER residency. Consistent with their colocalization, the potential of alt. UGT2B10 to interact with the UGT2B10 enzyme suggests that this may be a mechanism underlying their regulatory function.

The preferential stabilization of alt. isoforms by proteasomal inhibition and their shorter half-lives relative to the UGT2B10 enzyme suggest that distinct pathways may govern the turnover of alt. isoforms and the enzyme. This also suggests that a small variation in RNA levels has the potential to affect AS protein expression level. The significant abundance of alt. transcripts encoding these proteins may indicate that hepatic cells are poised to adapt levels of regulatory isoforms in response to various endogenous or exogenous stimuli. This is supported by the preferential mRNA expression of alternates in HepaRG cells treated with nuclear receptor agonists. Although the structural determinants of UGT protein stability are scarcely known, mechanisms modulating UGT turnover may significantly contribute to the regulation of their detoxifying functions, a well documented aspect for some drug-metabolizing cytochrome P450s (Zhukov and Ingelman-Sundberg, 1999; Kim et al., 2016 and references therein). When expressed in the HEK293 model, half-lives of UGTs were more than 12–16 hours for

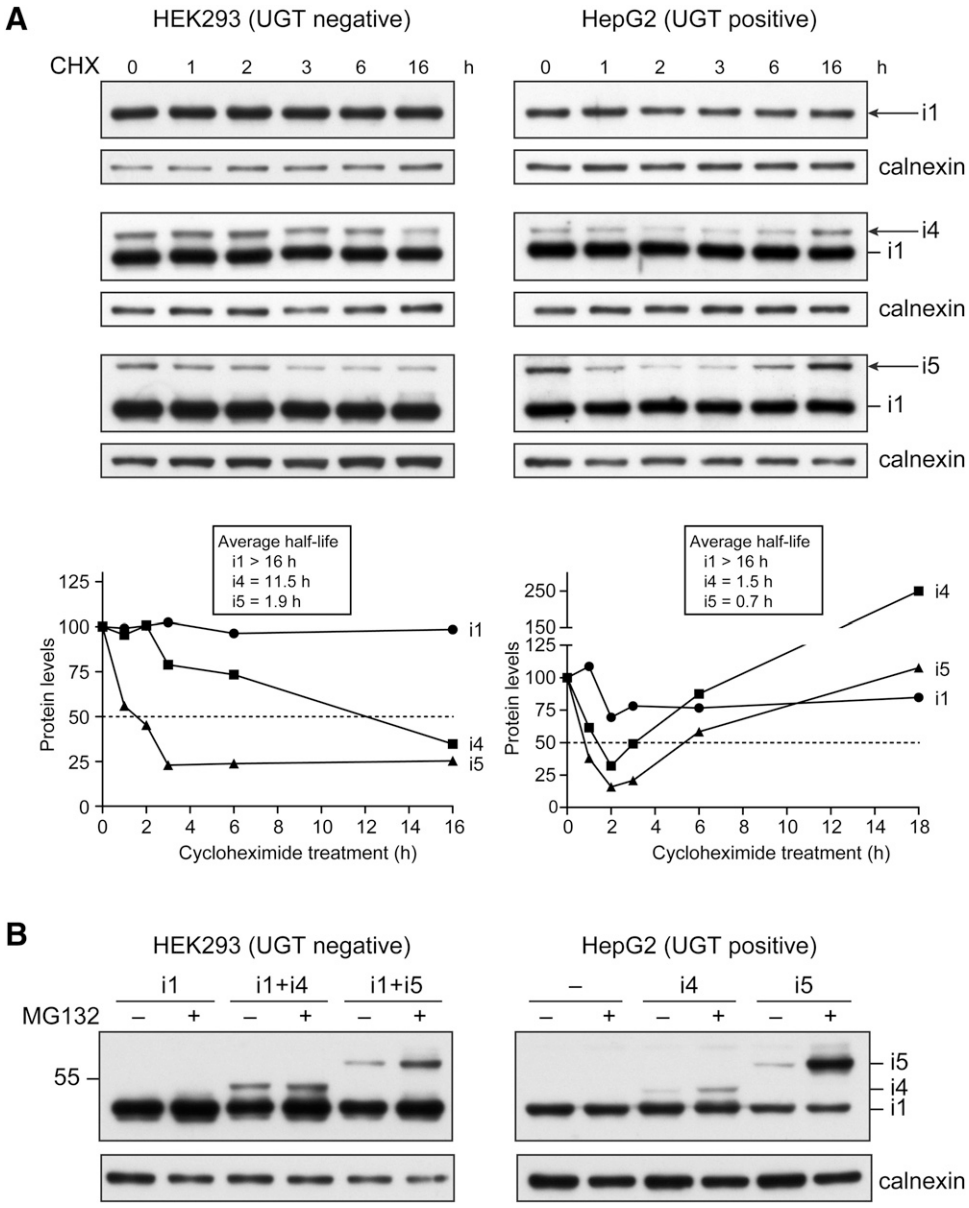

Fig. 6. Stability of UGT2B10 proteins. (A) The half-life of UGT2B10 proteins was determined by translational inhibition with cycloheximide (CHX) in HEK293 and HepG2 cell models. Protein levels were measured by densitometry scanning of immunoblots from two independent assays and are expressed as percentage of untreated cells. Half-lives were averaged from the two independent assays. A representative experiment is shown. An independent replicate assay is presented in Supplemental Fig. 4. (B) UGT2B10 alternative isoforms are stabilized by proteasomal inhibition. HEK293 and HepG2 cell models were exposed to vehicle only (dimethylsulfoxide; "−" lanes) or MG132 (1 μM; "+" lanes) for 16 hours. UGT2B10 was detected by immunoblotting total cell lysates (40 μg) with anti-UGT2B10.

UGT2B4, UGT2B7, UGT2B10, and UGT2B15, whereas UGT1A1 and UGT2B17 were more labile with half-lives less than 3 hours (Turgeon et al., 2001; Rouleau et al., 2016; this study). However, given that cycloheximide is glucuronidated by several UGT enzymes as demonstrated herein, alt. UGT protein half-lives established by translational inhibition with this compound in cells expressing UGTs likely constitute an inaccurate estimate that will be influenced by the enzymes expressed.

A limitation of our study is the lack of detection of alt. UGT2B10 by immunoblotting in pooled liver microsomes from 50 individuals using the polyclonal anti-UGT2B10 antibody #1845. Their expression varied widely among individuals (coefficient of variation of 155%), with some having no or barely detectable hepatic alt. *UGT2B10* variants. Levels of alt. proteins in our human liver pool may be too low for detection by immunoblotting. In contrast, the detection of alt. UGT2B10 by MS-MRM was performed following an immunoprecipitation step that enriched UGT2B10, thus improving the sensitivity of detection. The high turnover rate of the alt. proteins, as observed in the two cell models, may also influence our ability to detect them in human livers by immunoblotting. Additional experiments are required to ascertain the expression of alt. UGT2B10 proteins in individual human liver samples and their expression ratio relative to the UGT2B10 enzyme.

In conclusion, our study reveals that AS creates a diversified *UGT2B10* transcriptome and represents half of the UGT2B10 expression in the human liver, with a wide interindividual variability. Alternate UGT2B10 proteins may significantly influence the UGT2B10-dependent detoxification of amine-containing drugs, such as antipsychotic and tobacco metabolites, and are expected to modulate endogenous substrates of the UGT2B10 enzyme, which are currently unknown. Our study further highlights the long-term stability of the UGT2B10 enzyme that contrasts with the lability of alt. proteins, the latter being regulated by proteasomal degradation. Most interestingly, we further exposed a preferential induction by PXR and CAR inducers of alt. *UGT2B10* with novel in-frame C-terminal sequences in hepatic cells, implying a fine regulation of the AS process by xenosensing transcription factors. Our study highlights an important regulatory role of AS in UGT2B10 expression and detoxification functions that may explain part of the significant variability in N-glucuronidation, largely mediated by the UGT2B10 pathway in the liver. We thus believe that interindividual

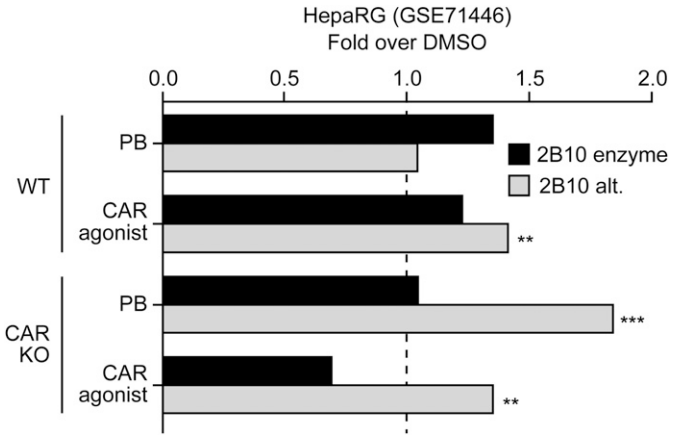

Fig. 7. Differential induction of alt. UGT2B10 by phenobarbital and a CAR agonist in HepaRG cells. Expression data for *UGT2B10* canonical and alt. transcripts *n9* and *n10* (encoding i4 and i5) in HepaRG cells, wild type (WT) or with a CAR knockout (KO), were obtained from the public RNA-seq data GSE71446. Cells were treated either with vehicle [dimethylsulfoxide (DMSO)], phenobarbital (PB; 1 mM), or the CAR agonist CITCO (1 μM) for 24 hours as previously described (Li et al., 2015). $^{**}P \leq 0.01$; $^{***}P \leq 0.001$.

differences in the clinical response to UGT2B10 substrates are likely to be understood through the AS process affecting both the constitutive and inducible expression of UGT2B10.

Acknowledgments

We thank Dr. H. Wang and B. Mackowiak (University of Maryland) for their collaboration with the HepaRG data, and Patrick Caron, Véronique Turcotte, Anne-Marie Duperré, Camille Girard-Bock, and Andréa Fournier for their technical assistance. We also thank the Proteomics Platform of the CHU de Québec Research Center for their services.

Authorship Contributions

Participated in research design: Labriet, Allain, Rouleau, Audet-Delage, Guillemette.

Conducted experiments: Labriet, Allain, Audet-Delage, Villeneuve.

Performed data analysis: Labriet, Allain, Rouleau, Audet-Delage, Villeneuve, Guillemette.

Wrote or contributed to the writing of the manuscript: Labriet, Rouleau, Guillemette.

References

Anthérieu S, Chesné C, Li R, Guguen-Guillouzo C, and Guillouzo A (2012) Optimization of the HepaRG cell model for drug metabolism and toxicity studies. *Toxicol In Vitro* **26**:1278–1285.

Barré L, Magdalou J, Netter P, Fournel-Gigleux S, and Ouzzine M (2005) The stop transfer sequence of the human UDP-glucuronosyltransferase 1A determines localization to the endoplasmic reticulum by both static retention and retrieval mechanisms. *FEBS J* **272**:1063–1071.

Beaulieu M, Lévesque E, Hum DW, and Bélanger A (1998) Isolation and characterization of a human orphan UDP-glucuronosyltransferase, UGT2B11. *Biochem Biophys Res Commun* **248**:44–50.

Bellemare J, Rouleau M, Girard H, Harvey M, and Guillemette C (2010a) Alternatively spliced products of the UGT1A gene interact with the enzymatically active proteins to inhibit glucuronosyltransferase activity in vitro. *Drug Metab Dispos* **38**:1785–1789.

Bellemare J, Rouleau M, Harvey M, and Guillemette C (2010b) Modulation of the human glucuronosyltransferase UGT1A pathway by splice isoform polypeptides is mediated through protein-protein interactions. *J Biol Chem* **285**:3600–3607.

Berg JZ, Mason J, Boettcher AJ, Hatsukami DK, and Murphy SE (2010) Nicotine metabolism in African Americans and European Americans: variation in glucuronidation by ethnicity and UGT2B10 haplotype. *J Pharmacol Exp Ther* **332**:202–209.

Bolger AM, Lohse M, and Usadel B (2014) Trimmomatic: a flexible trimmer for Illumina sequence data. *Bioinformatics* **30**:2114–2120.

Bray NL, Pimentel H, Melsted P, and Pachter L (2016) Near-optimal probabilistic RNA-seq quantification. *Nat Biotechnol* **34**:525–527.

Bushey RT and Lazarus P (2012) Identification and functional characterization of a novel UDP-glucuronosyltransferase 2A1 splice variant: potential importance in tobacco-related cancer susceptibility. *J Pharmacol Exp Ther* **343**:712–724.

Chen G, Blevins-Primeau AS, Dellinger RW, Muscat JE, and Lazarus P (2007) Glucuronidation of nicotine and cotinine by UGT2B10: loss of function by the UGT2B10 Codon 67 (Asp>Tyr) polymorphism. *Cancer Res* **67**:9024–9029.

Chen G, Dellinger RW, Gallagher CJ, Sun D, and Lazarus P (2008a) Identification of a prevalent functional missense polymorphism in the UGT2B10 gene and its association with UGT2B10 inactivation against tobacco-specific nitrosamines. *Pharmacogenet Genomics* **18**:181–191.

Chen G, Dellinger RW, Sun D, Spratt TE, and Lazarus P (2008b) Glucuronidation of tobacco-specific nitrosamines by UGT2B10. *Drug Metab Dispos* **36**:824–830.

Chen G, Giambrone NE, and Lazarus P (2012) Glucuronidation of trans-3′-hydroxycotinine by UGT2B17 and UGT2B10. *Pharmacogenet Genomics* **22**:183–190.

Chhibber A, French CE, Yee SW, Gamazon ER, Theusch E, Qin X, Webb A, Papp AC, Wang A, Simmons CQ, et al. (2016) Transcriptomic variation of pharmacogenes in multiple human tissues and lymphoblastoid cell lines. *Pharmacogenomics J* **17**:137–145.

Chouinard S, Pelletier G, Bélanger A, and Barbier O (2006) Isoform-specific regulation of uridine diphosphate-glucuronosyltransferase 2B enzymes in the human prostate: differential consequences for androgen and bioactive lipid inactivation. *Endocrinology* **147**:5431–5442.

Ciotti M, Cho JW, George J, and Owens IS (1998) Required buried alpha-helical structure in the bilirubin UDP-glucuronosyltransferase, UGT1A1, contains a nonreplaceable phenylalanine. *Biochemistry* **37**:11018–11025.

Court MH, Zhang X, Ding X, Yee KK, Hesse LM, and Finel M (2012) Quantitative distribution of mRNAs encoding the 19 human UDP-glucuronosyltransferase enzymes in 26 adult and 3 fetal tissues. *Xenobiotica* **42**:266–277.

de Jonge HJ, Fehrmann RS, de Bont ES, Hofstra RM, Gerbens F, Kamps WA, de Vries EG, van der Zee AG, te Meerman GJ, and ter Elst A (2007) Evidence based selection of housekeeping genes. *PLoS One* **2**:e898.

Fallon JK, Neubert H, Hyland R, Goosen TC, and Smith PC (2013) Targeted quantitative proteomics for the analysis of 14 UGT1As and -2Bs in human liver using NanoUPLC-MS/MS with selected reaction monitoring. *J Proteome Res* **12**:4402–4413.

Fowler S, Kletzl H, Finel M, Manevski N, Schmid P, Tuerck D, Norcross RD, Hoener MC, Spleiss O, and Iglesias VA (2015) A UGT2B10 splicing polymorphism common in african populations may greatly increase drug exposure. *J Pharmacol Exp Ther* **352**:358–367.

Girard-Bock C, Benoit-Biancamano MO, Villeneuve L, Desjardins S, and Guillemette C (2016) A rare UGT2B7 variant creates a novel N-glycosylation site at codon 121 with impaired enzyme activity. *Drug Metab Dispos* **44**:1867–1871.

Guillemette C, Lévesque E, Harvey M, Bellemare J, and Menard V (2010) UGT genomic diversity: beyond gene duplication. *Drug Metab Rev* **42**:24–44.

Guillemette C, Lévesque É, and Rouleau M (2014) Pharmacogenomics of human uridine diphospho-glucuronosyltransferases and clinical implications. *Clin Pharmacol Ther* **96**:324–339.

Haakensen VD, Biong M, Lingjærde OC, Holmen MM, Frantzen JO, Chen Y, Navjord D, Romundstad L, Lüders T, Bukholm IK, et al. (2010) Expression levels of uridine 5′-diphospho-glucuronosyltransferase genes in breast tissue from healthy women are associated with mammographic density. *Breast Cancer Res* **12**:R65.

Jackson MR, Nilsson T, and Peterson PA (1993) Retrieval of transmembrane proteins to the endoplasmic reticulum. *J Cell Biol* **121**:317–333.

Jones NR and Lazarus P (2014) UGT2B gene expression analysis in multiple tobacco carcinogen-targeted tissues. *Drug Metab Dispos* **42**:529–536.

Kaivosaari S, Finel M, and Koskinen M (2011) N-glucuronidation of drugs and other xenobiotics by human and animal UDP-glucuronosyltransferases. *Xenobiotica* **41**:652–669.

Kaivosaari S, Toivonen P, Aitio O, Sipilä J, Koskinen M, Salonen JS, and Finel M (2008) Regio- and stereospecific N-glucuronidation of medetomidine: the differences between UDP glucuronosyltransferase (UGT) 1A4 and UGT2B10 account for the complex kinetics of human liver microsomes. *Drug Metab Dispos* **36**:1529–1537.

Kaivosaari S, Toivonen P, Hesse LM, Koskinen M, Court MH, and Finel M (2007) Nicotine glucuronidation and the human UDP-glucuronosyltransferase UGT2B10. *Mol Pharmacol* **72**:761–768.

Kato Y, Izukawa T, Oda S, Fukami T, Finel M, Yokoi T, and Nakajima M (2013) Human UDP-glucuronosyltransferase (UGT) 2B10 in drug N-glucuronidation: substrate screening and comparison with UGT1A3 and UGT1A4. *Drug Metab Dispos* **41**:1389–1397.

Kazmi F, Barbara JE, Yerino P, and Parkinson A (2015) A long-standing mystery solved: the formation of 3-hydroxydesloratadine is catalyzed by CYP2C8 but prior glucuronidation of desloratadine by UDP-glucuronosyltransferase 2B10 is an obligatory requirement. *Drug Metab Dispos* **43**:523–533.

Kerdpin O, Mackenzie PI, Bowalgaha K, Finel M, and Miners JO (2009) Influence of N-terminal domain histidine and proline residues on the substrate selectivities of human UDP-glucuronosyltransferase 1A1, 1A6, 1A9, 2B7, and 2B10. *Drug Metab Dispos* **37**:1948–1955.

Kim SM, Wang Y, Nabavi N, Liu Y, and Correia MA (2016) Hepatic cytochromes P450: structural degrons and barcodes, posttranslational modifications and cellular adapters in the ERAD-end-game. *Drug Metab Rev* **48**:405–433.

Lépine J, Bernard O, Plante M, Têtu B, Pelletier G, Labrie F, Bélanger A, and Guillemette C (2004) Specificity and regioselectivity of the conjugation of estradiol, estrone, and their catecholestrogen and methoxyestrogen metabolites by human uridine diphospho-glucuronosyltransferases expressed in endometrium. *J Clin Endocrinol Metab* **89**:5222–5232.

Lévesque E, Beaulieu M, Green MD, Tephly TR, Bélanger A, and Hum DW (1997) Isolation and characterization of UGT2B15(Y85): a UDP-glucuronosyltransferase encoded by a polymorphic gene. *Pharmacogenetics* **7**:317–325.

Li D, Mackowiak B, Brayman TG, Mitchell M, Zhang L, Huang SM, and Wang H (2015) Genome-wide analysis of human constitutive androstane receptor (CAR) transcriptome in wild-type and CAR-knockout HepaRG cells. *Biochem Pharmacol* **98**:190–202.

Lu D, Wang S, Xie Q, Guo L, and Wu B (2017a) Transcriptional Regulation of Human UDP-Glucuronosyltransferase 2B10 by Farnesoid X Receptor in Human Hepatoma HepG2 Cells. *Mol Pharm* **14**:2899–2907.

Lu D, Xie Q, and Wu B (2017b) N-glucuronidation catalyzed by UGT1A4 and UGT2B10 in human liver microsomes: assay optimization and substrate identification. *J Pharm Biomed Anal* **145**:692–703.

Lu L, Zhou J, Shi J, Peng XJ, Qi XX, Wang Y, Li FY, Zhou FY, Liu L, and Liu ZQ (2015) Drug-metabolizing activity, protein and gene expression of UDP-glucuronosyltransferases are significantly altered in hepatocellular carcinoma patients. *PLoS One* **10**:e0127524.

Margaillan G, Rouleau M, Klein K, Fallon JK, Caron P, Villeneuve L, Smith PC, Zanger UM, and Guillemette C (2015) Multiplexed targeted quantitative proteomics predicts hepatic glucuronidation potential. *Drug Metab Dispos* **43**:1331–1335.

Ménard V, Collin P, Margaillan G, and Guillemette C (2013) Modulation of the UGT2B7 enzyme activity by C-terminally truncated proteins derived from alternative splicing. *Drug Metab Dispos* **41**:2197–2205.

Murphy SE (2017) Nicotine metabolism and smoking: ethnic differences in the role of P450 2A6. *Chem Res Toxicol* **30**:410–419.
Murphy SE, Park SS, Thompson EF, Wilkens LR, Patel Y, Stram DO, and Le Marchand L (2014) Nicotine N-glucuronidation relative to N-oxidation and C-oxidation and UGT2B10 genotype in five ethnic/racial groups. *Carcinogenesis* **35**:2526–2533.
Ohno S and Nakajin S (2011) Quantitative analysis of UGT2B28 mRNA expression by real-time RT-PCR and application to human tissue distribution study. *Drug Metab Lett* **5**:202–208.
Ouzzine M, Magdalou J, Burchell B, and Fournel-Gigleux S (1999) An internal signal sequence mediates the targeting and retention of the human UDP-glucuronosyltransferase 1A6 to the endoplasmic reticulum. *J Biol Chem* **274**:31401–31409.
Patel YM, Stram DO, Wilkens LR, Park SS, Henderson BE, Le Marchand L, Haiman CA, and Murphy SE (2015) The contribution of common genetic variation to nicotine and cotinine glucuronidation in multiple ethnic/racial populations. *Cancer Epidemiol Biomarkers Prev* **24**:119–127.
Pattanawongsa A, Nair PC, Rowland A, and Miners JO (2016) Human UDP-glucuronosyltransferase (UGT) 2B10: validation of cotinine as a selective probe substrate, inhibition by UGT enzyme-selective inhibitors and antidepressant and antipsychotic drugs, and structural determinants of enzyme inhibition. *Drug Metab Dispos* **44**:378–388.
Radominska-Pandya A, Bratton SM, Redinbo MR, and Miley MJ (2010) The crystal structure of human UDP-glucuronosyltransferase 2B7 C-terminal end is the first mammalian UGT target to be revealed: the significance for human UGTs from both the 1A and 2B families. *Drug Metab Rev* **42**:133–144.
Rath A, Glibowicka M, Nadeau VG, Chen G, and Deber CM (2009) Detergent binding explains anomalous SDS-PAGE migration of membrane proteins. *Proc Natl Acad Sci USA* **106**: 1760–1765.
Risso D, Schwartz K, Sherlock G, and Dudoit S (2011) GC-content normalization for RNA-Seq data. *BMC Bioinformatics* **12**:480.
Risso D, Ngai J, Speed TP, and Dudoit S (2014) Normalization of RNA-seq data using factor analysis of control genes or samples. *Nature Biotechnology* **32**:896.
Rouleau M, Roberge J, Bellemare J, and Guillemette C (2014) Dual roles for splice variants of the glucuronidation pathway as regulators of cellular metabolism. *Mol Pharmacol* **85**:29–36.
Rouleau M, Tourancheau A, Girard-Bock C, Villeneuve L, Vaucher J, Duperré AM, Audet-Delage Y, Gilbert I, Popa I, Droit A, et al. (2016) Divergent expression and metabolic functions of human glucuronosyltransferases through alternative splicing. *Cell Reports* **17**:114–124.
Sato Y, Nagata M, Tetsuka K, Tamura K, Miyashita A, Kawamura A, and Usui T (2014) Optimized methods for targeted peptide-based quantification of human uridine 5′-diphosphate-glucuronosyltransferases in biological specimens using liquid chromatography-tandem mass spectrometry. *Drug Metab Dispos* **42**:885–889.
Tourancheau A, Margaillan G, Rouleau M, Gilbert I, Villeneuve L, Lévesque E, Droit A, and Guillemette C (2016) Unravelling the transcriptomic landscape of the major phase II UDP-glucuronosyltransferase drug metabolizing pathway using targeted RNA sequencing. *Pharmacogenomics J* **16**:60–70.
Tourancheau A, Rouleau M, Guauque-Olarte S, Villeneuve L, Gilbert I, Droit A, and Guillemette C (2017) Quantitative profiling of the UGT transcriptome in human drug-metabolizing tissues. *Pharmacogenomics J* DOI: 10.1038/tpj.2017.5 [published ahead of print].
Turgeon D, Carrier JS, Lévesque E, Hum DW, and Bélanger A (2001) Relative enzymatic activity, protein stability, and tissue distribution of human steroid-metabolizing UGT2B subfamily members. *Endocrinology* **142**:778–787.
Turgeon D, Chouinard S, Belanger P, Picard S, Labbe JF, Borgeat P, and Belanger A (2003) Glucuronidation of arachidonic and linoleic acid metabolites by human UDP-glucuronosyltransferases. *J Lipid Res* **44**:1182–1191.
Ware JJ, Chen X, Vink J, Loukola A, Minica C, Pool R, Milaneschi Y, Mangino M, Menni C, Chen J, et al. (2016) Genome-wide meta-analysis of cotinine levels in cigarette smokers identifies locus at 4q13.2. *Sci Rep* **6**:20092.
Zhou D, Guo J, Linnenbach AJ, Booth-Genthe CL, and Grimm SW (2010) Role of human UGT2B10 in N-glucuronidation of tricyclic antidepressants, amitriptyline, imipramine, clomipramine, and trimipramine. *Drug Metab Dispos* **38**:863–870.
Zhukov A and Ingelman-Sundberg M (1999) Relationship between cytochrome P450 catalytic cycling and stability: fast degradation of ethanol-inducible cytochrome P450 2E1 (CYP2E1) in hepatoma cells is abolished by inactivation of its electron donor NADPH-cytochrome P450 reductase. *Biochem J* **340**:453–458.

Address correspondence to: Dr. Chantal Guillemette, Pharmacogenomics Laboratory, Centre Hospitalier Universitaire de Québec Research Center, Université Laval, 2705 Boul. Laurier, R4701.5, Québec, Canada, G1V 4G2. E-mail: Chantal.Guillemette@crchudequebec.ulaval.ca